RSC Advances

ROYAL SOCIETY OF CHEMISTRY

www.rsc.org/advances

An Electrochemical sensor for determination of Tryptophan in the presence of DA based on poly(L-Methionine)/ Graphene modified electrode

Yingzi Wang, Xiaoqian Ouyang, Yaping Ding*, Bingdi Liu, Duo Xu, Lanfeng Liao

Department of Chemistry, Shanghai University, Shanghai 200444, P R China

Abstract: A glassy carbon electrode modified with poly(L-Methionine) and graphene composite film(PLME/GR/GCE) was fabricated by electropolymerization for determination of L-tryptophan (L-Trp) in the presence of dopamine(DA). The morphology and structure of the composite film were investigated by scanning electron microscopy (SEM), fourier transform infrared spectroscopy (FT-IR), raman spectroscopy and electrochemical impedance spectroscopy (EIS). Differential pulse voltammetry (DPV) was utilized to investigate the electrocatalytical oxidation of L-Trp from the potentially interfering species on the PLME/GR/GCE. Under optimum conditions, the proposed method exhibited wide linear dynamic range 0.2−150 μM, with a detection limit (S/N=3), and good reproducibility and high selectivity. Moreover, the proposed modified electrode has been successfully applied to determine L-Trp in milk and human serum samples.

Keywords: Tryptophan; Poly(L-Methionine); Graphene

* Corresponding author. Tel.: +86 21 66134734; Fax: +86 21 66132797.

Address: Department of Chemistry, Shanghai University, Shanghai 200444, PR China.

E-mail address: wdingyp@sina.com (Y.P. Ding)

1. Introduction

L-Tryptophan (Trp) is one of the most important essential amino acids having biochemical, nutritional and clinical significance in humans and herbivores.[1] It is a derivative of alanine with an indole substituent on the β carbon.[2] The substituted indole rings are widely used in biochemistry. Trp is one of the indispensable amino acids since our body cannot synthesize it from other compounds through chemical reactions. It is commonly synthesized in plants and microorganisms from shikimic acid.[3] Trp is abundantly present in oats, milk, chocolates, bananas, yogurt, dried dates, etc. as component of dietary protein while it is scarcely present in vegetables. Apart from playing a pivotal role in the production of nervous system messengers, it acts as a precursor for many neurotransmitters and neurochemicals, including serotonin and melatonin.[4-5] Melatonin is known to help improve sleep, and serotonin is needed to improve mood and mental health.[6] Dopamine (DA) is also a kind of neurotransmitters, which is found in whole human body and brain the same with Trp. The connection of those two is an important part in psychiatry. Simultaneous determination of Trp and DA is important, since both occur together in biological systems. The Trp supplements have been used for some time as antidepressants, sleep aids and weigh-loss aids. Improper metabolism of Trp accumulates toxic products in brain which causes hallucinations, delusions and schizophrenia.[7] An overdose of Trp creates drowsiness, nausea, dizziness and loss of appetite.[8] Meanwhile, DA system plays a central role in important medical conditions including Parkinson's disease, attention deficit hyperactivity disorder, schizophrenia, and drug addiction. Therefore, it is relevant to develop a simple, fast, inexpensive and accurate method for the

determination of Trp in food products, pharmaceuticals and biological fluids in the presence of DA and is likely to have great significance in life science research and drug analysis.

Some methods have been developed for the determination of Trp and DA including, chromatographic methods,[9] chemiluminescence,[10] capillary electrophoresis[11] and electrochemical methods[12]. Among these methods, owing to Trp and DA taking part in complex biochemical reactions are electroactive, electrochemical techniques, with high sensitivity, high accuracy and simple operation, have been paid much more attention in recent years. However, the electrochemical detection of Trp faces some problems. At traditional working electrodes, Trp oxidation suffers from high overpotential and sluggish kinetics.[13] Chemically modified electrodes have been constructed to overcome the problem, such as Au-NPs/GCE,[14] GNP/CILE,[6] MCPE/MWCNTs,[15] MWCNT-LDH-CPE,[2] Poly(4-aminobenzoic acid)/GCE,[16] poly-sulfosalicylic acid/GCE[17]. Among these electrodes, polymer film modified electrodes have been paid great attention due to their good stability, biocompatibility, homogeneity , strong adherence to electrode surface.[18,19] Studies have indicated that polymer film modified electrodes show an enhanced response for the determination of various important biological and clinical species[20-22] owing to the ability to provide a platform to selective recognition.[23] The thickness, permeation and charge transport characteristics of the polymeric films can be controlled by the potential and current applied.

As we know, graphene (GR) has attracted intense attention since its discovery in

2004.[24] The graphene has perfect conductivity which can amplify electrochemical signal,[23] because of its fascinating two-dimensional structure, unusual electrochemical properties, large accessible surface area, as well as good biocompatibility.[25,26]

In short, the synergy of graphene and polymer leads to successful and effective recognition tryptophan. Those two materials can be modified compactly and homogeneously on the surface GCE owing to the electrostatic interactions. Thus, the composite film is applied to the electrochemical tryptophan, and the graphene combined polymer modified on GCE can be evaluated by electrochemical methods revealed a higher L-Trp affinity.[27]

In this paper, L-Methionine (LME) was chosen as a monomer to form a polymer modified film. It is one of the sulfur-containing proteinogenic amino acids and governs the main supply of sulfur in the diet, and also prevents disorders in hair and skin. Thus, we have fabricated a PLME/GR/GCE modified electrode by electro-polymerization. The modified electrode was characterized by electrochemical impedance spectroscopy and scanning electron microscopy, and it was applied to the electrocatalytic oxidation of L -tryptophan (L-Trp) by differential pulse voltammetry (DPV). The process was simple and fast. Moreover, the modified electrode showed excellent electrocatalytic properties in determination of L-Trp, making it suitable for the analytical purpose.

2. Experimental

2.1 Reagents and apparatus

L-Trp, L-Methionine and DA were supplied from obtained from Sinopharm

Chemical Reagent Co., Ltd. (Shanghai, China). Graphene was purchased from XFNANO, INC (Nanjing, China). Phosphate buffer solutions (PBS, 0.1 M) with different pH values were prepared by mixing stock solution of 0.1 M K_2HPO_4, 0.1 M KH_2PO_4 and 0.1 M H_3PO_4 (Shanghai Chemical Reagent Co., Ltd., China). All chemicals were of analytical grade and used without further purification.

All electrochemical experiments were carried out on a CHI 660C electrochemical workstation (Shanghai Chenhua Co., Ltd., China) with a conventional three-electrode system consisting of a PLME modified glassy carbon electrode, a saturated calomel reference electrode and a Pt foil counter electrode. The pH value was determined with a pHS-3C acidity meter. Scanning electron micrographs (SEM) were carried out using a scanning electron microscope (JSM-6700F, 15.0 kV). Fourier transform infrared (FTIR) spectra were carried out on a Fourier transform infrared spectrometer (AVATAR 370, America). Raman scattering was performed on an INVIA (England) Raman Microscope using a 545.5 nm laser source.

2.2 Preparation of PLME/GR/GCEC

Prior to modification, the GCE was polished on chamois leather with 0.05 μm α-alumina powder, thoroughly rinsed with water and sonicated in 1:1 (v/v) HNO_3, absolute alcohol and doubly distilled water in turn. The GR/GCE was gained via electro-deposition by applying a potentiostatic potential of +1.8 V in 0.1 M KCl containing 200 mL 1 mg mL^{-1} GR.[28,29] Electropolymerization of L-Methionine on the GR/GCE was carried out by 5 circles in 0.1 M PBS (pH 6.0) containing 1mM

L-Methionine. The parameters of this method were set as follows: potential range, -0.8-2.1 V; scan rate, 100 mV/s; sample interval, 1 mV; sweep segment, 10; quiet time, 2s.All experimental procedures were performed at room temperature. Then PLME/GR/GCE was fabricated. Electrochemical response of L-Trp at bare GCE, GCE modified with L-Methionine alone (PLME/GCE) and GR/GCE were also followed for comparison.

3. Results and discussion

3.1 Characterization of modified electrode

3.1.1 SEM, FTIR and Raman spectroscopy

Fig. 1A shows the SEM image of graphene and 1B illustrates poly L-Methionine on the surface of GCE. It defines that each monomer granules uniformly dispersed in the surface of GCE. In Fig. 1C, because of the different configuration, it shows the composite film has been successfully modified on the surface of GCE.

<Fig. 1 here>

Fig. 2A illustrates the FTIR spectra of the monomer methionine (a) and poly(methionine) (b). As show in curve a, it can be seen peaks of C-H stretching vibration (2918 cm^{-1}), N-H stretching vibration (3449 cm^{-1}), O-H stretching vibration (2609 cm^{-1}), C-S stretching vibration (536 cm^{-1}).These peaks are assigned to characteristic absorption of methionine. As shown in curve b, it can be seen that the peaks of 2111 cm^{-1} disappeared because the peaks of N-H became weak and the peaks in fingerprint region become broader after polymerization.[30] This was caused by the

poly-reaction of methionine, indicating that the PLME film has been formed.

Raman spectroscopy is a powerful nondestructive tool to distinguish ordered and disordered crystal structures of carbon. The G-band, which originates from the first-order scattering from the doubly degenerate E_{2g} phonon modes of graphite in the Brillouin zone center, is characteristic of all sp^2-hybridized carbon networks, while the prominent D peak is a breathing mode of *k*-point phonons of A_{1g} symmetry, assigned to structural imperfections created by the attachment of oxygenated groups on the carbon basal plane.[31-33] Thus, the intensity ratio of the D and G bands (ID/IG) offers not only clues to the oxidation degree and the size of sp^2 ring clusters in a network of sp^3 and sp^2 bonded carbon,[34] but also the degree of defects and disorder of the graphitized structures.[35,36] Fig. 2B presents the Raman spectra of bare GCE, GR/GCE and PLME/GR/GCE with a distinguished changing of D/G intensity ratio. Specifically, the intensity ratio decrease from 1.815 of bare GCE to 1.093 of GR/GCE. After the modification of PLME onto GR, the intensity ratio was 1.052 and a weak peak appeared at 1753 cm^{-1}. The two prominent peaks of the D and G bands also shifted from 1328.3 and 1600.9 cm^{-1} of bare GCE to 1323.0 and 1601.9 cm^{-1} of GR/GCE, and 1340.4 and 1605.4 cm^{-1} of PLME/GR/GCE.

<Fig. 2 here>

3.1.2 Electrochemical study of PLME/GR/GCE

Electrochemical impedance spectroscopy (EIS) was used as an efficient tool to characterize the interface properties of the electrode surfaces. The electron-transfer

resistance (R_{et}) at the electrode surface corresponds to the semicircle diameter of the Nyquist plots.[37] As shown in Fig. 3A, the diameter of the semicircular part of PLME/GR/GCE was smaller than PLME/GCE and GR/GCE. This indicated that the PLME/GR film greatly improves the conductivity and the electron transfer process. Fig. 3B shows cyclic voltammograms in 0.1 M KCl containing 5.0 mM $[Fe(CN)_6]^{3-/4-}$at bare GCE, GR/GCE, PLME/GCE and PLME/GR/GCE. For PLME/GR/GCE, the peak current became larger than PLME/GCE and GR/GCE. This may be attributed to the combination of GR and PLME increased the surface area and conductivity of film. The peak current of PLME/GR/GCE was smaller than bare GCE, may be caused by the thickness of the modified film.

<Fig. 3 here>

3.2 Electrochemical behavior of modified electrode

The electrochemical behavior of modified electrode in the presence of L-Trp was investigated by differential pulse voltammograms (DPV). The parameters of this method were set as follows: potential range, 0.4-1.1 V; Potential increments, 0.004 V; pulse period, 0.5 s; sample width, 0.0167 s; quiet time, 20 s. All experimental procedures were performed at room temperature. Fig. 4 displays the DPV of the electrochemical oxidation of 10 μM L-Trp in 0.1 M PBS (pH 2.5) at bare GCE (a), PLME/GCE (b), GR/GCE (c) and PLME/GR/GCE (d). As for the bare GCE, the oxidation peak of L-Trp was weak, and the oxidation peak of L-Trp appeared at 0.82 V. At the PLME/GCE, the oxidation current of L-Trp was larger, and the oxidation peak

appeared shifted negatively to 0.80 V. After compositing the PLME and GR film, the oxidation current of L-Trp became larger and the oxidation peak appeared at 0.76 V, demonstrating that the combination of the PLME and GR helps enhance the kinetics of the electrochemical process as an efficient promoter.

<Fig. 4 here>

3.3 Effect of operational parameters

3.3.1 Effect of pH values

The relationship between pH and peak currents of L-Trp is illustrated in Fig. 5a. It can be seen that the oxidation peak currents decreased gradually with the pH from 2.0 to 10.0. As shown in Fig. 5a, the maximum currents was achieved when the pH increase to 2.5, and decreased when the pH was less than 2.5, we choose 2.5 for further experiments.

The pH value of the supporting electrolyte is an important factor that affects the electrochemical reactions of analytes. Fig. 5b represents the oxidation peak potential (E_{pa}) of 10 μM L-Trp at PLME/GR/GCE shifted negatively with the increase of pH associated with a proton-transfer process. Linear dependence between potentials and pH for L-Trp was obtained as follows:

$$E_{pa}\ (V) = 0.9134 - 0.0498\ pH\ (R=0.9997).$$

The slope of the equation is -49.8mV/pH, which is in agreement with the ideal state 59mV/pH(25℃). The result shows that the number of proton equals that of electron in the reaction.

<Fig. 5 here>

3.3.2 Effect of electro-polymerization cycles

The effect of the electro-polymerization cycles of PLME on the oxidation currents of 10 μM L-Trp was investigated by DPV. As shown in Fig. 6, the maximum currents was achieved when the cycles are set to 5, and decreased when the cycles was larger than 5. This may be associated with the thickness of the PLME film. Therefore, the electro-polymerization cycles of 5 was selected.

<Fig. 6 here>

3.3.3 Effect of scan rate

The cyclic voltammograms of 10 μM L-Trp on the PLME/GR/GCE at various scan rates (10–200 mV) are shown in Fig. 7. The insets demonstrate the relationship of the oxidation peak currents (I_{pa}) with the scan rates. It can be seen that, the oxidation currents of L-Trp was linearly proportional to the square roots of scan rates in the range of 10−200 mV s^{-1}, indicating that reactions of L-Trp on PLME/GR/GCE were diffusion-controlled process. In addition, the oxidation peak potential (E_{pa}) shifts to more positive values with the increase of scan rates, which suggests that the electron transfer is quasi-reversible.

To further characterize the kinetic parameters, the influence of the scan rate on the redox peak potential (E_{pa}) for L-Trp was also investigated by CV methods. This is according to the Laviron method.[38] The method predicts a linear relationship between

*E*pa and the logarithm of scan rate (log v). On the basis of Laviron's model, the relationship between the potential and the scan rate can be expressed as follow.

$$E_{pa} = E^{0`} + \frac{2.3RT}{(1-\alpha)nF}\log v$$

In Fig. 7B, it can be observed that the oxidation peak potential shifted positively with the increase of scan rate, and the E_{pa} showed a linear dependence with log v. The linear regression equation for L-Trp is as follow

$$E_{pa}\ (V) = 0.8089 + 0.0267 \log v\ (V\ s^{-1},\ R = 0.9987)$$

Generally, the electron-transfer coefficient (α) is around 0.4-0.6.[39] Assuming the electron-transfer coefficient to be 0.6 for an irreversible electrode process. Accordingly, the electron-transfer number (n) can be calculated: for L-Trp is 1.85, which is in agreement with previously reported result.

<Fig. 7 here>

Hence, the overall oxidation process of L-Trp involves two electrons and two protons as shown in Scheme 1. Our results are consistent with the mechanism reported in the literature.

<Scheme. 1 here>

3.4 Calibration curve and interferences

Under the optimum conditions, the electrochemical behaviors of different concentrations of L-Trp were studied. As shown in Fig. 8, the change of DPVs indicates that the oxidative peak current (I_{pa}) has linear relationship with the concentration (c) of L-Trp. In the range from 4.0×10^{-8} to 1.0×10^{-5} M, a linear

243 regression equations:

244 I_{pa}=0.1147+0.312c (μM) (R=0.9953)

245 was obtained, with the detection limit (S/N = 3) and the sensitivity was
246 calculated to be 0.017μM and 23.4 μA mM^{-1} cm^{-2}, respectively. Table 1 summarizes
247 the analytical results of the proposed method and comparison with other
248 electrochemical methods reported previously for detecting L-Trp. It can be seen that
249 the electrochemical performance of our method is comparable to the literature
250 methods.

251 <Fig. 8 here>

252 <Table 1>

253

254 In addition, DA is an important biological substance which often coexists with
255 L-Trp in biological samples. To evaluate the influence of DA on the determination of
256 L-Trp, DA was added into 0.1 M PBS containing L-Trp for determination. Fig. 9
257 displays the DPV of different concentration of L-Trp in 0.1 M PBS containing 5 μM
258 DA. The peak currents increased synchronously with concentrations of L-Trp,
259 implying that PLME/GR/GCE can be also applied for the simultaneous determination
260 of L-Trp in the presence of DA. A linear regression range was obtained：

261 I_{pa} =−0.0041+0.5095c (μM) (R=0.995) (0.2−10 μM);

262 I_{pa} =4.8955+0.0451 c (μM) (R=0.995) (10−150 μM).

263 <Fig. 9 here>

264

To investigate other possible interferences for the detection of L-Trp, various foreign species were added into 0.1 M PBS (pH 2.5) containing 10 μM L-Trp. Table 2 shows the signal change of different potential interferences for the determination of 10 μM L-Trp. It was found that no significant interference (signal change <5%) for these compounds: NaCl (500 μM), KNO_3(500μM), $ZnSO_4$(500μM), $NHCl_4$(500μM), L-Glucose(500 μM), L-Threonine (500 μM), L-Serine (500 μM), L-Alanine (500 μM), L-Asparagic acid (500 μM), L-Leucine (100 μM), Ascorbic acid (250 μM), dopamine (100μM) and UA (100μM).

<Table 2 here>

3.5 Reproducibility and stability

In order to evaluate the precision of this method, a series of repetitive voltammetric measurements were carried out at the same PLME/GR/GCE. The relative standard deviations (R.S.D.) for seven successive determinations of 10μM L-Trp was 1.40%, indicating an excellent detecting reproducibility. The storage stability of PLME/GR/GCE was also investigated. After the modified electrode stored in the refrigerator for two weeks, the result shows that the catalytic current response maintains 99.6%, and after stored for 30 days, the catalytic current response maintains 89.7%, illustrating the good stability of the proposed sensor.

3.6 Real Samples analysis

Human serum samples and milk were selected as real samples for ananlysis by

the propose method. Both the serum samples and milk was diluted 5 times. The diluted serum sample (20 μL) was directly added into 10 mL of 0.1 PBS (pH 2.5). The diluted milk (20μL) was injected into the same PBS solution. Both the solutions were analyzed by the standard addition method for three times. The results were listed in Table 3. The good recoveries of the samples indicate that the developed sensor is applicable to the determination of L-Trp in real samples.

<Table 3 here>

4. Conclusions

A convenient, rapid and stable biosensor for voltammetric determination of L-tryptophan was developed by modifying the GCE with poly(L-Methionine) and graphene composite film. The PLME/GR modified electrode is easy to prepare and exhibited excellent electrocatalytic activity for L-Trp in the presence of DA. By this simple method of fabrication, a much lower detection limit was achieved without involving any pre-treatment or activation steps. Moreover, the analytical applicability of the modified electrode has been evaluated by successfully employing it for the determination of L-Trp in the blood serum and milk.

5. Acknowledgements

This work is supported by the National Natural Science Foundation of China (No. 21271127, 61171033), the Nano-Foundation of Science and Techniques Commission of Shanghai Municipality (No. 12nm0504200, 12dz1909403).

References

[1] H. Wang, H. Cui, A. Zhang and R. Liu, *Analytical Communications*, 1996, **33**, 275–277.

[2] O.J. D'Souza, R.J. Mascarenhas, T. Thomas, I.N.N. Namboothiri, M. Rajamathi, P. Martis and J. Dalhalle, *Journal of Electroanalytical Chemistry*. 2013, **704**, 220–226.

[3] A.A. Ensafi, H.K. Maleh and S. Mallakpour, *Electroanalysis,* 2012, **24**, 666–675.

[4] D. Ye, L. Luo, Y. Ding, B. Liu and X. Liu, *Analyst*, 2012, **137**, 2840–2845.

[5] K. Palme, F. Nagy, *Cell*, 2008, **133**, 31–32.

[6] A. Safavi, S. Momeni, *Electroanalysis*, 2010, **22**, 2848 – 2855

[7] R.N. Goyal, S. Bishnoi, H. Chasta, M.A. Aziz, M. Oyama, *Talanta*, 2011, **85**, 2626–2631.

[8] A. Ozcan, Y. Sahin, *Biosensors and Bioelectronics*, 2012, **31**, 26–31.

[9] E. Kojima, M. Kai and Y. Ohkura, *Journal of Chromatography A*, 1993, **612**, 90–187.

[10] G.N. Chen, R.E. Lin, Z.F. Zhao, *Analytica Chimica Acta*, 1997, **341**, 251–256.

[11] A. Zinellu, S. Sotgia and L. Deiana, *Journal of Separation Science*. 2012, **35**, 1146–1151.

[12] G.P. Jin, X.Q. Lin, *Electrochemistry Communications*, 2004, **6**, 60–454.

[13] Z. Zhang, S.Q. Gu, Y.P. Ding, J.D. Jin and F.F. Zhang, *Analytical Methods*, 2013, **5**, 4859–4864.

[14] C.Y. Li, Y. Ya and G.Q. Zhan, *Colloids and Surfaces B: Biointerfaces*, 2010, **76**,

340–345.

[15] T. Thomas, R.J. Mascarenhas, O.J. D'Souza, P. Martis, J. Dalhalle and B.E. Kumara Swamy, *Journal of Colloid and Interface Science*, 2013, **402**, 223–229.

[16] K.J. Huang, C.X. Xu, W.Z. Xie and W. Wang, *Colloids and Surfaces B: Biointerfaces*, 2009, **74** ,167–171.

[17] X. Ba, L.Q. Luo, Y.P. Ding and X. Liu, *Sensors and Actuators B: Chemical*, 2013, **187**, 27–32.

[18] F. Bedioui, J. Devynck and C. Bied-Charreton, *Accounts of Chemical Research*, 1995, **28**, 30–36.

[19] B.I. Podlovchenko, V.N. Andreev, *Russian Chemical Reviews*, 2002, **71**, 837–851.

[20] M.E. Ghica, C.M.A. Brett, *Talanta*, 2014, **130**, 198–206.

[21] M. Taei, G. Ramazani, *Colloids and Surfaces B: Biointerfaces*, 2014, **123**, 23–32.

[22] H.M. Abdolhamid, G. Nasrin, A.K. Mohammad, G. Masoumeh and I.R. Somaieh, *Electroanalysis*, 2014, **26**, 2491–2500.

[23] J. Ou, Y.X. Tao, J.J. Xue, Y. Kong, J.Y. Dai and L.H. Deng, *Electrochemistry Communications*, 2015, **57**, 5-9.

[24] K.S. Novoselov, A.K. Geim, S.V. Morozov, D. Jiang, Y. Zhang, S.V. Dubonos, I.V. Grigorieva and A.A. Firsov, *Science*, 2004, **306**, 666–669.

[25] X. Wang, C. Wang, K. Qu, Y. Song, J. Ren, D. Miyoshi, N. Sugimoto and X. Qu, *Advanced Functional Materials,* 2010, **20**, 3967–3971.

[26] A.K. Geim, K.S. Novoselov, *Nature Materials*, 2007, **6**, 183–191.

[27] J. Ou, Y.H. Zhu, Y. Kong, J.F. Ma, *Electrochemistry Communications*, 2015, **60**, 60-63.

[28] L. Jiang, S.Q. Gu, Y.P. Ding, F. Jiang and Z. Zhang, *Nanoscale*, 2014, **6**, 207-214.

[29] X.Q. Ouyang, L.Q. Luo, Y.P. Ding, B.D. Liu and D. Xu, *Journal of Electroanalytical Chemistry*, 2014, **735**, 51–56.

[30] W.H. Qiao, L. Wang, B.X. Ye, G.P. Li and J.J. Li, *Analyst*, 2015, **140**, 7974–7983.

[31] D. Yang, A. Velamakanni, G. Bozoklu, S. Park, M. Stoller, R. D. Piner, S. Stankovich, I. Jung, D. A. Field and C.A. Ventrice, *Carbon*, 2009, **47**, 145–152.

[32] M. A. Pimenta, G. Dresselhaus, M.S. Dresselhaus, L.G. Cancado, A. Jorio and R. Saito, *Physical Chemistry Chemical Physics*, 2007, **9**, 1276–1291.

[33] M. S. Dresselhaus, G. Dresselhaus, M. Hoffmann and Philos, Philosophical, *Transactions of The Royal Society A*, 2008, **366**, 231–236.

[34] C. Mattevi, G. Eda, S. Agnoli, S. Miller, K.A. Mkhoyan, O. Celik, D. Mastrogiovanni, G. Granozzi, E. Garfunkel and M. Chhowalla, *Advanced Functional Materials*, 2009, **19**, 2577–2583.

[35] D. Graf, F. Molitor, K. Ensslin, C. Stampfer, A. Jungen, C. Hierold and L. Wirtz, *Nano Letters*, 2007, **7**, 238–242.

[36] F. Tuinstra, J. L. Koenig, *The Journal of Chemical Physics*, 1969, **53**, 1126–1130.

[37] G. Pelossof, R. Tel-Vered, S. Shimron and I. Willner, *Chemical Science*, 2013, **4**, 1137–1144.

376 [38] Y. H. Huang, J. H. Chen, L. J. Ling, Z. B. Su, X. Sun, S. R. Hu, W. Weng, Y.
377 Huang, W. B. Wu and Y. S. He, *Analyst*, 2015, **140**, 7939–7949.
378 [39] O. J. D'Souza, R. J. Mascarenhas, A. K. Satpati, I. N. N. Namboothiri, S.
379 Detriche, Z. Mekhalif and J. Delhallee, RSC Advance, 2015, **5**, 91472–91481.
380 [40] J.B. Raoof, R. Ojani, M. Baghayeri, *Sensors and Actuators B: Chemical*, 2009,
381 **143**, 261–269.
382 [41] H.X. Li, Y. Wang, D.X. Ye, J. Luo, B.Q. Su, S. Zhang and J.L. Kong, *Talanta*,
383 2014, **127**, 255–261.
384 [42] C. Wang, R. Yuan, Y.Q. Chai, S.H. Chen, F.X. Hu and M.H. Zhang, *Analytica*
385 *Chimica Acta*, 2012, **741**, 15–20.
386 [43] A. Babaei, E. Ansari, M. Afrasiabi, *Analytical Methods*, 2014, **6**, 8729–8737.
387

Figure Captions:

Fig. 1 SEM of GR/GCE (a), PLME/GCE (b) and PLME/GR/GCE (c)

Fig. 2 (A) Fourier transforms infrared spectra of L-Methionine (a) and poly(L-Methionine) (b), (B) Raman spectra of bare GCE, GR/GCE and PLME/GR/GCE

Fig. 3 Electrochemical impedance spectra (a) and cyclic voltammograms (b) of bare GCE, GR/GCE, PLME/GCE and PLME/GR/GCE in 0.1 M KCl containing 5 mM $[Fe(CN)_6]^{3-/4-}$ at the scan rate of 100 mV s^{-1}

Fig. 4 DPVs for 10 μM L-Trp in 0.1 M PBS (pH 2.5) at bare GCE (a), GR/GCE (b), PLME/GCE (c), and PLME/GR/GCE (d)

Fig. 5 Influence of pH on the difference of the peak potentials (a) and the peak currents (b) obtained from DPV for 10 μM L-Trp at the PLME/GR/GCE modified electrodes

Fig. 6 Effect of electro-polymerization cycles of L-Methionine on the oxidation current response of 10 μM L-Trp at PLME/GR/GCE in 0.1 PBS (pH 2.5)

Fig. 7 Cyclic voltammograms (CVs) of 10 μM L-Trp in 0.1 M PBS (pH 2.5) at PLME/GR/GCE at different scan rate (10-200 mV/s). Inset: plots of Ipa vs. square root of scan rate (A) and the relationship between oxidation peak potentials of L-Trp and scan rate (B)

Fig. 8 DPVs of determination of L-Trp (0.04-10 μM) using PLME/GR/GCE in 0.1 M PBS (pH 2.5). Inset: plots of Ip vs. concentrations of L-Trp

Fig. 9 DPVs of determination of L-Trp (0.2-150 μM) in the presence of 10 μM DA

using PLME/GR/GCE in 0.1 M PBS (pH 2.5). Inset: plots of Ip vs. concentrations of L-Trp

Table Captions:

Table 1 Comparison of analytical performance of L-Trp on PLME/GR/GCE with other modified electrodes in the literature

Table 2 The influences of some organic ions and important biological substances on the peak currents of 10 μM L-Trp in 0.1 M PBS (pH 2.5)

Table 3 Determination of L-Trp in human serum and milk samples

420 **Scheme Captions:**

421 **Scheme 1** Oxidation mechanism of L-Trp at PLME/GR/GCE

Fig. 1 (A) SEM of GR/GCE (a), PLME/GCE (b) and PLME/GR/GCE (c)

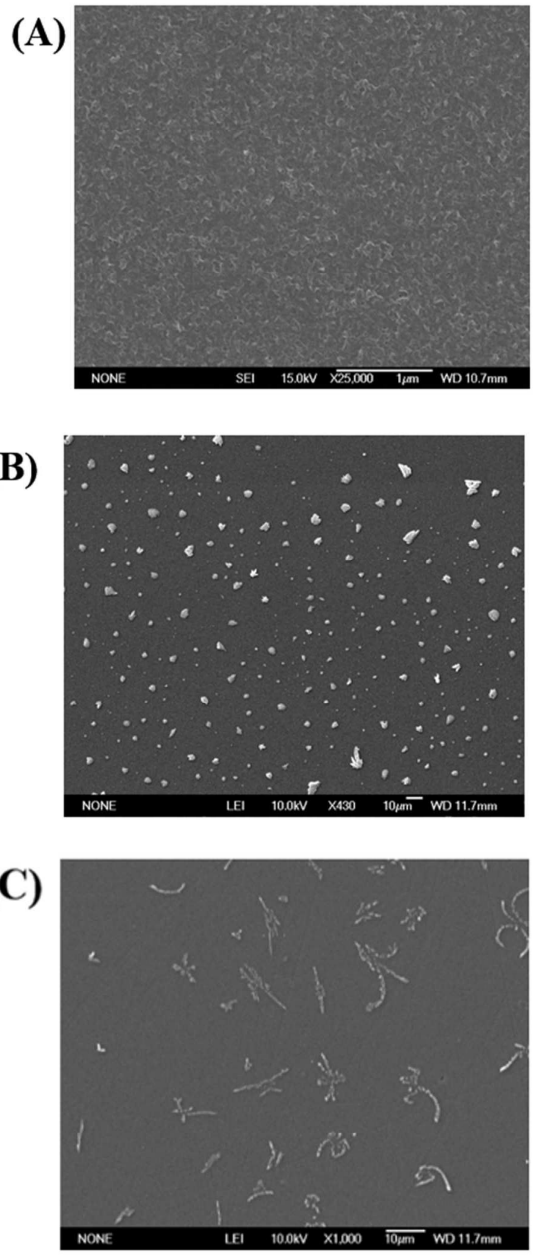

Fig. 2 (A) Fourier transforms infrared spectra of L-Methionine (a) and poly (L-Methionine) (b), (B) Raman spectra of bare GCE, GR/GCE and PLME/GR/GCE

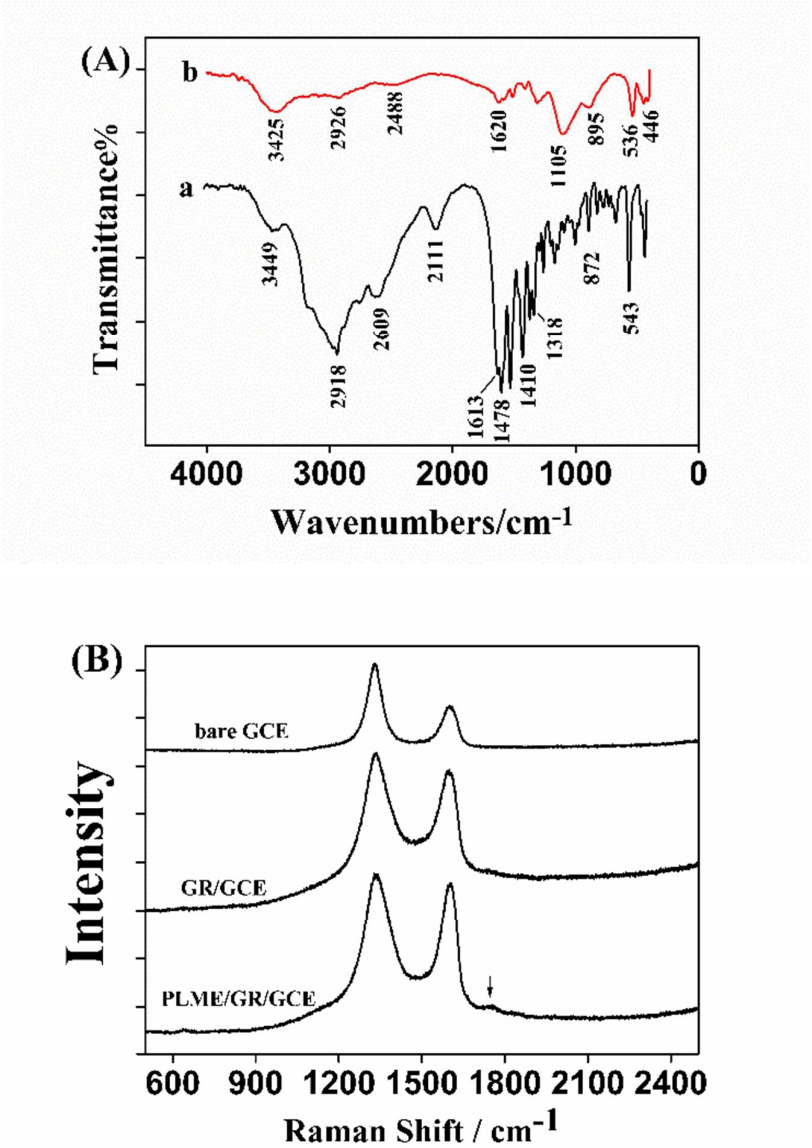

Fig. 3 Electrochemical impedance spectra (a) and cyclic voltammograms (b) of bare GCE, GR/GCE, PLME/GCE and PLME/GR/GCE in 0.1 M KCl containing 5 mM $[Fe(CN)_6]^{3-/4-}$ at the scan rate of 100 mV s^{-1}

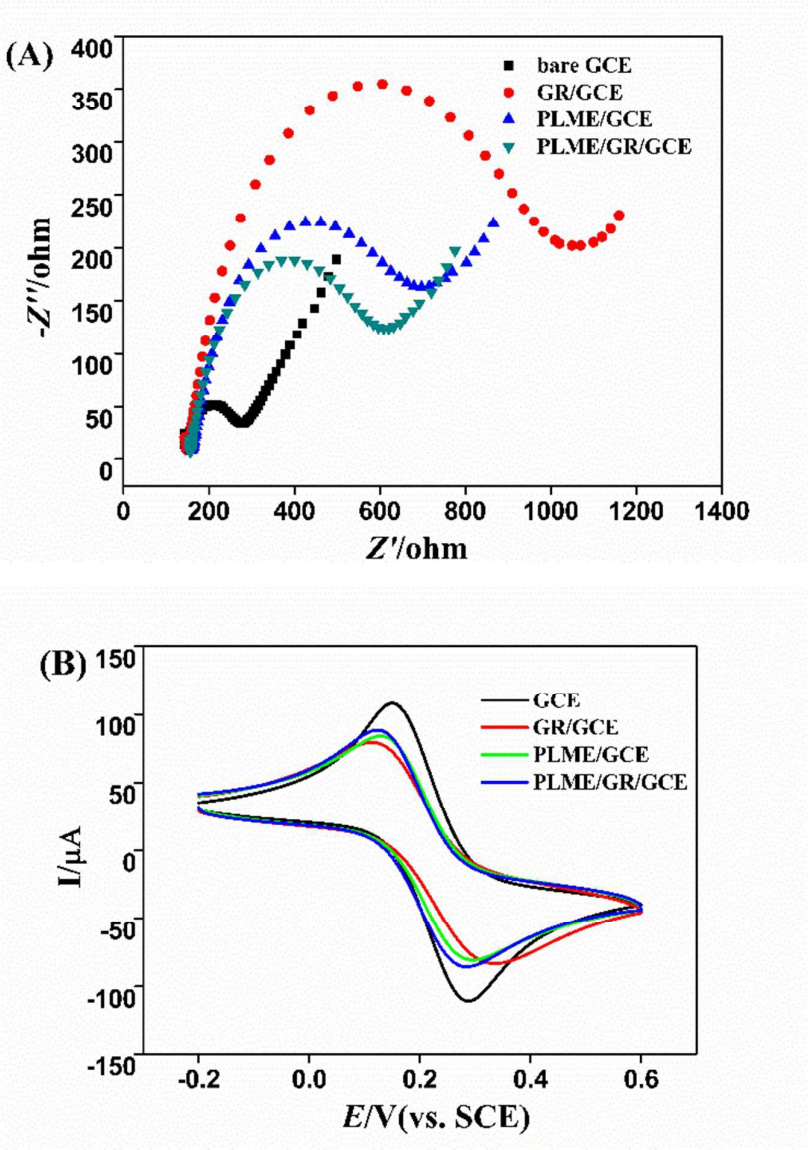

Fig. 4 DPVs for 10 μM L-Trp in 0.1 M PBS (pH 2.5) at bare GCE (a), GR/GCE (b), PLME/GCE (c), and PLME/GR/GCE (d)

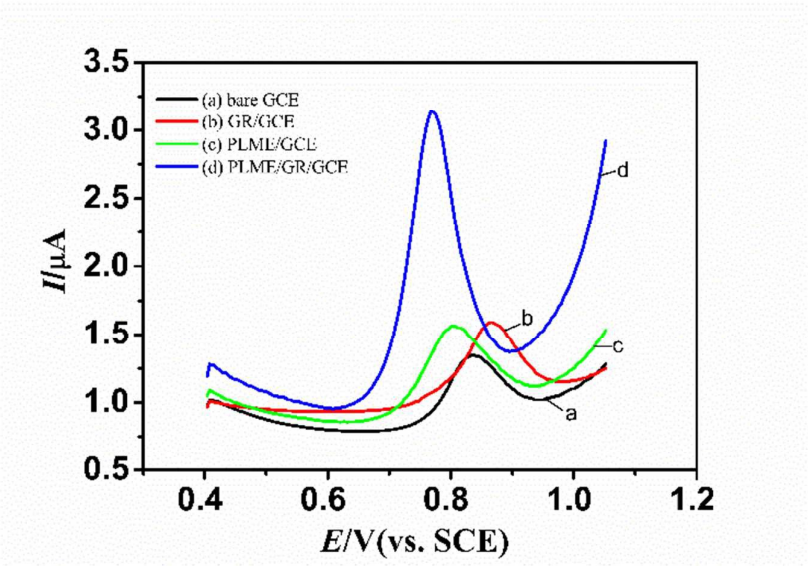

Fig. 5 Influence of pH on the difference of the peak currents (A) and the peak potentials (B) obtained from DPV for 10 Mm L-Trp at the PLME/GR/GCE modified electrodes

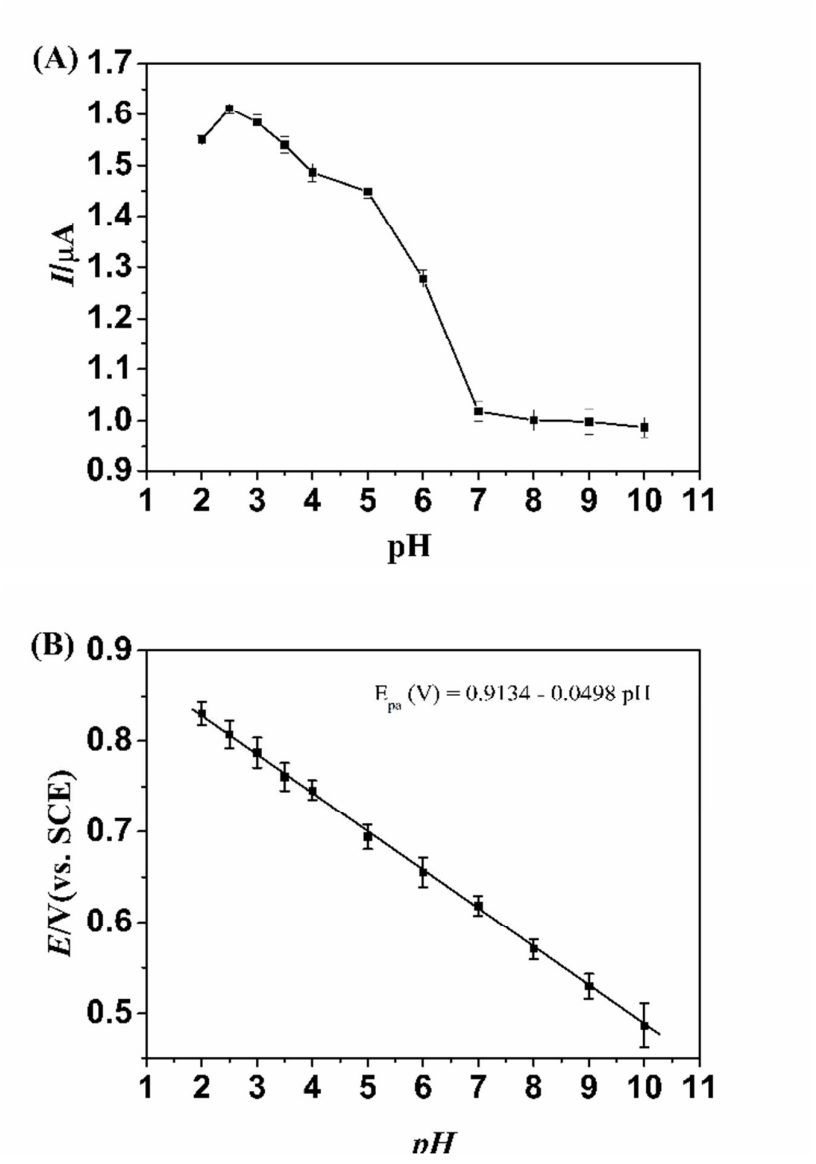

Fig. 6 Effect of electro-polymerization cycles of L-Methionine on the oxidation current response of 10 μM L-Trp at PLME/GR/GCE in 0.1 PBS (pH 2.5)

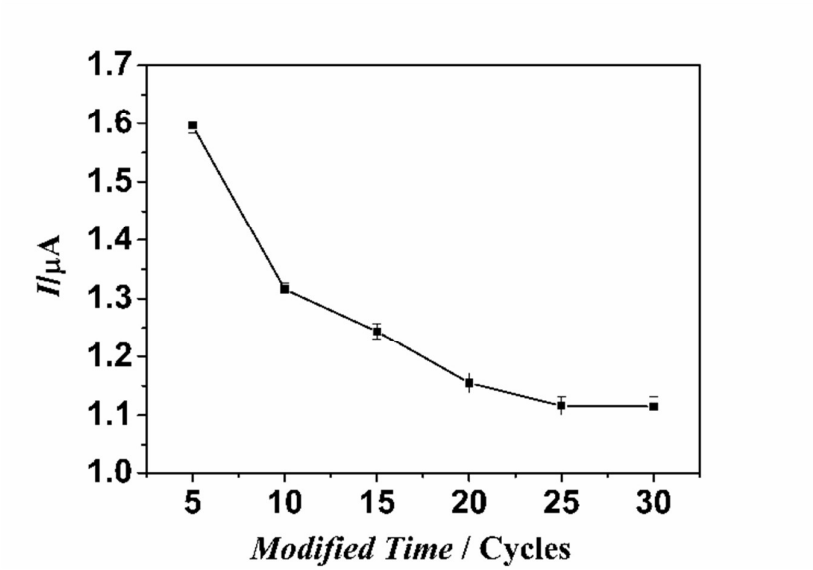

Fig. 7 Cyclic voltammograms (CVs) of 10 μM L-Trp in 0.1 M PBS (pH 2.5) at PLME/GR/GCE at different scan rate (10-200 mV/s). Inset: plots of Ip_a vs. square root of scan rate (A) and the relationship between oxidation peak potentials of L-Trp and scan rate (B)

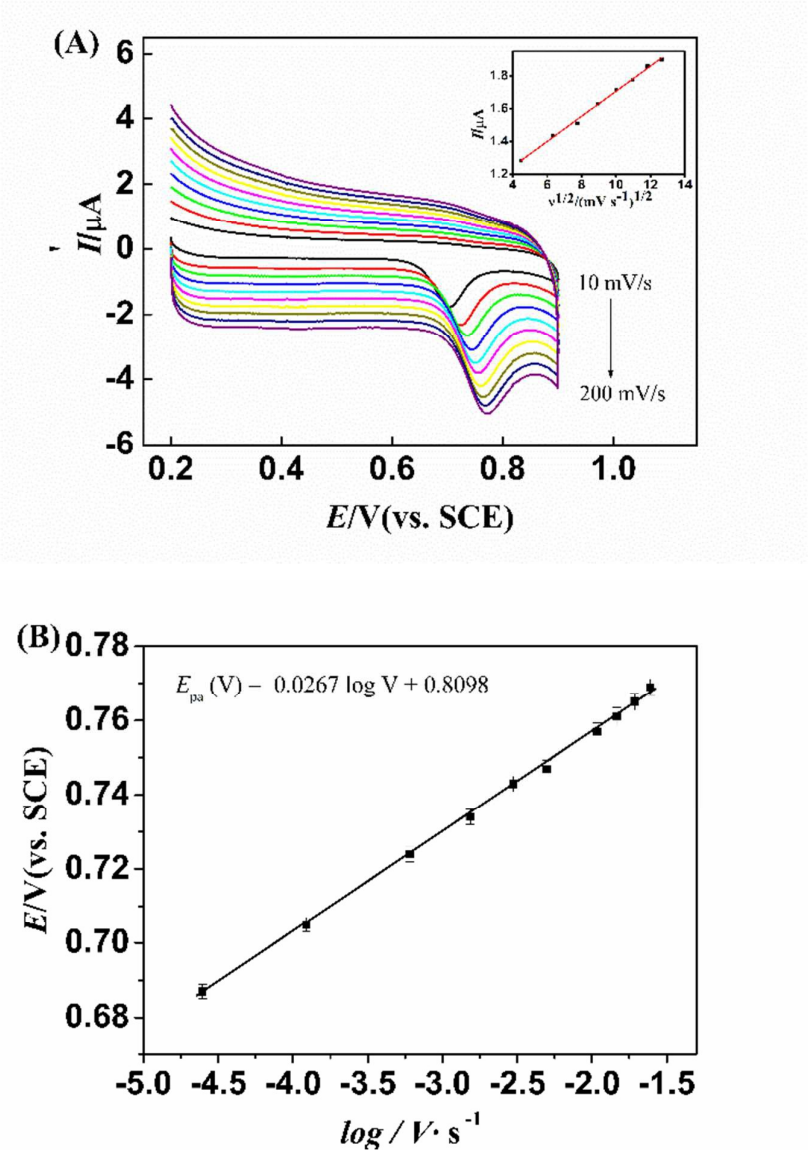

Fig. 8 DPVs of determination of L-Trp (0.04-10 μM) using PLME/GR/GCE in 0.1 M PBS (pH 2.5). Inset: plots of I_{pa} vs. concentrations of L-Trp

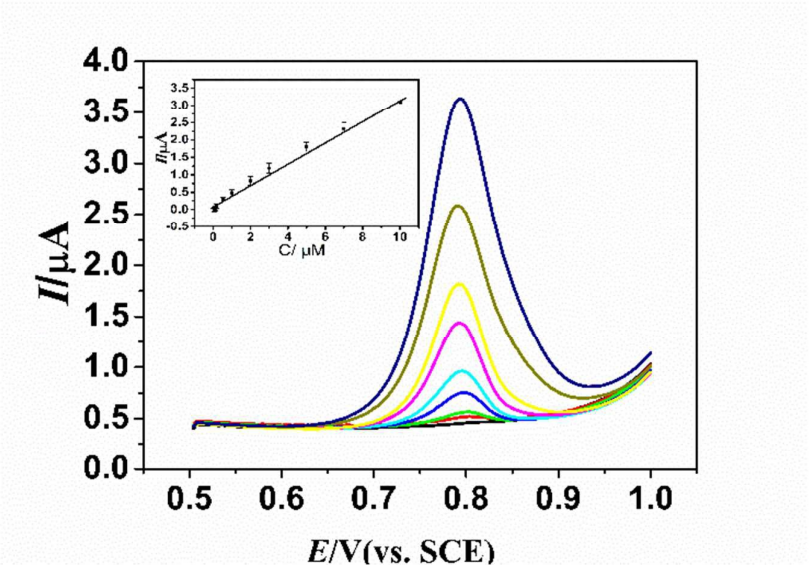

Fig. 9 DPVs of determination of L-Trp (0.2-150 μM) in the presence of 10 μM DA using PLME/GR/GCE in 0.1 M PBS (pH 2.5). Inset: plots of Ip_a vs. concentrations of L-Trp

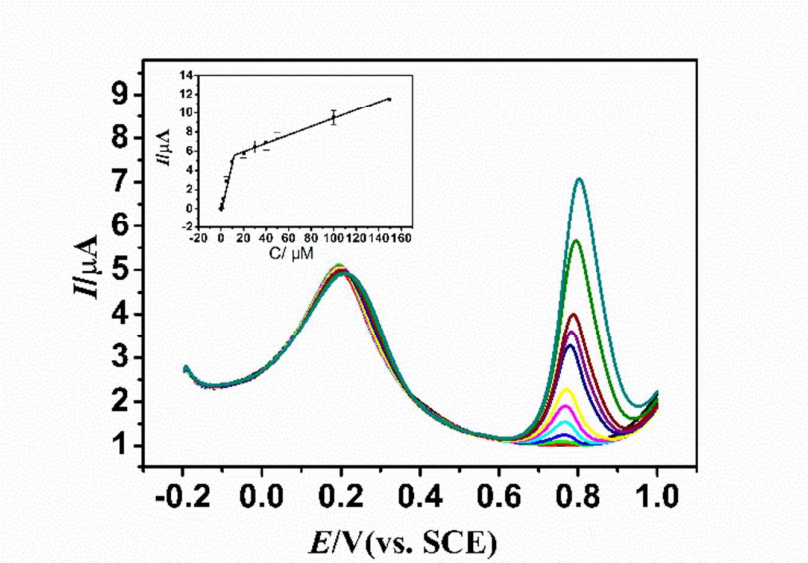

Table 1 Comparison of analytical performance of L-Trp on PLME/GR/GCE with other modified electrodes in the literature

Electrode	Dynamic ranges (μM)	Detection limits (μM)	References
poly(4-aminobenzoic acid) GCE	1.0-100	0.2	[16]
CILE/GNP	5.0-900	4.0	[6]
MWNTs/Mg–Al/CPE	3-9 9-1000	0.0068	[2]
nano-TiO_2/FCCa /CPE	0.4-14	0.124	[38]
MWNTs/GS/GCE	5-30 60-500	0.87	[39]
GNPs/PImox	3-464	0.70	[40]
MWCNTs–NHNPs–MCM-41/GCE	0.5-50	0.11	[41]
PLME/GR/GCE	0.05-10	0.017	This work

Table 2 The influences of some organic ions and important biological substances on the peak currents of 10 μM L-Trp in 0.1 M PBS (pH 2.5)

Interferences	Concentration(μM)	Signal change
		L-Trp
Na^+	500	–4.80%
K^+	500	–3.34%
Zn^{2+}	500	–0.50%
Mg^{2+}	500	–4.13%
NH_4^+	500	–4.90%
Cl^-	500	–4.80%
NO_3^-	500	–3.34%
SO_4^{2-}	500	–0.50%
D-Glucose	500	–4.60%
L- Threonine	500	–4.90%
L- Serine	500	–4.80%
L- Alanine	500	–4.00%
Asparagic acid	500	–4.30%
Leucine	100	–3.38%
Ascorbic acid	250	2.90%
Dopamine	100	2.75%

Table 3 Determination of L-Trp in human serum and milk samples

Samples	Detected (μM)	Added (μM)	Found (μM)	Recovery
Serum 1	-	0.50	0.48	96.7%
	-	1.00	1.04	103.9%
	-	1.50	1.54	103.1%
	-	3.00	3.14	104.7%
Milk		0.5	0.51	103.0%
		1.0	0.97	97.0%
	-	1.5	1.49	99.3%
	-	3.0	3.12	104.0%

1 **Scheme 1** Oxidation mechanism of L-Trp at PLME/GR/GCE

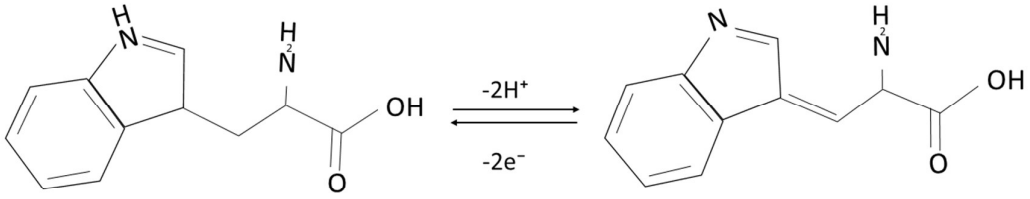

2

Graphical Abstract

Electrocatalytic oxidation of L-Trp at poly(L-Methionine)/graphene composite film modified glassy carbon electrode (PLME/GR/GCE) were investigaed by differential pulse voltammetry.

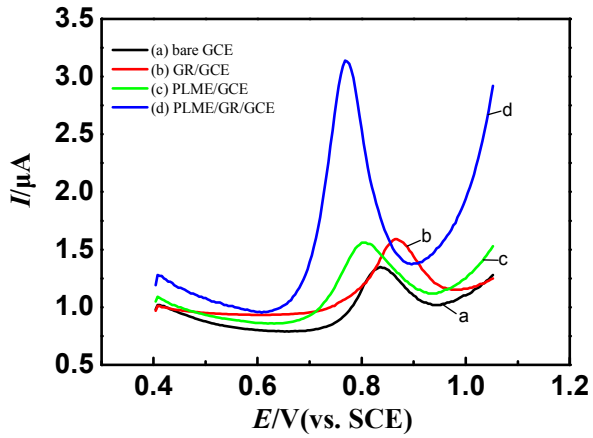

DPVs for 10 μM Trp in 0.1 M PBS (pH 2.5) at bare GCE (a), GR/GCE (b), PLME/GCE (c), and PLME/GR/GCE (d)